

Elimination of Purkinje Fibers by Electroporation Reduces Ventricular Fibrillation Vulnerability

Christopher Livia, BS;* Alan Sugrue, MBBCh;* Tyra Witt, CVT; Murray D. Polkinghorne, MBChB; Elad Maor, MD, PhD; Suraj Kapa, MD; Helge I. Lehmann, MD; Christopher V. DeSimone, MD, PhD; Atta Behfar, MD, PhD; Samuel J. Asirvatham, MD; Christopher J. McLeod, MBChB, PhD

Background—The Purkinje network appears to play a pivotal role in the triggering as well as maintenance of ventricular fibrillation. Irreversible electroporation (IRE) using direct current has shown promise as a nonthermal ablation modality in the heart, but its ability to target and ablate the Purkinje tissue is undefined. Our aim was to investigate the potential for selective ablation of Purkinje/fascicular fibers using IRE.

Methods and Results—In an ex vivo Langendorff model of canine heart (n=8), direct current was delivered in a unipolar manner at various dosages from 750 to 2500 V, in 10 pulses with a 90- μ s duration at a frequency of 1 Hz. The window of ventricular fibrillation vulnerability was assessed before and after delivery of electroporation energy using a shock on T-wave method. IRE consistently eradicated all Purkinje potentials at voltages between 750 and 2500 V (minimum field strength of 250–833 V/cm). The ventricular electrogram amplitude was only minimally reduced by ablation: 0.6 ± 2.3 mV ($P=0.03$). In 4 hearts after IRE delivery, ventricular fibrillation could not be reinduced. At baseline, the lower limit of vulnerability to ventricular fibrillation was 1.8 ± 0.4 J, and the upper limit of vulnerability was 19.5 ± 3.0 J. The window of vulnerability was 17.8 ± 2.9 J. Delivery of electroporation energy significantly reduced the window of vulnerability to 5.7 ± 2.9 J ($P=0.0003$), with a postablation lower limit of vulnerability= 7.3 ± 2.63 J, and the upper limit of vulnerability= 18.8 ± 5.2 J.

Conclusions—Our study highlights that Purkinje tissue can be ablated with IRE without any evidence of underlying myocardial damage. (*J Am Heart Assoc.* 2018;7:e009070. DOI: 10.1161/JAHA.118.009070.)

Key Words: ablation • direct current ablation • irreversible electroporation • Purkinje fibers • ventricular fibrillation • window of vulnerability

Ventricular fibrillation (VF) is a terminal cardiac dysrhythmia in humans,^{1,2} occurring either as a primary or a secondary event to concomitant cardiac and noncardiac diseases. Currently, there is no cure for VF, with only

rudimentary treatment options available; thus, sudden cardiac death from VF remains a major worldwide health problem.^{3,4} The Purkinje system is implicated in the genesis of primary VF,^{5–7} with radiofrequency ablation successfully treating this lethal arrhythmia by targeting triggers, such as a premature ventricular beat emanating from Purkinje tissue.^{7–10} However, current radiofrequency ablation approaches to the Purkinje fibers have limitations, particularly because they can only be applied in a point-to-point manner, which is tedious and time-consuming. Chemical denudation of the Purkinje system has been attempted and shown to lower the VF threshold,¹¹ but results in acute toxicity to the heart.

Direct current (DC) applied in a pulsed manner can cause permeation of the cellular membrane, a process known as electroporation. Depending on the electric field (V/cm) applied, the effect of electroporation can be transient, and tissue remains viable after electric field exposure (termed reversible electroporation). Conversely, when the cells are exposed to a prolonged electric field, resulting in permanent permeabilization of the cell and subsequent disruption of homeostasis, the cells will die, and the term irreversible

From the Department of Cardiovascular Medicine and Department of Molecular Pharmacology and Experimental Therapeutics, Center for Regenerative Medicine (C.L., T.W., A.B.), Division of Heart Rhythm Services, Department of Cardiovascular Diseases (A.S., M.D.P., S.K., H.I.L., C.V.D., S.J.A., C.J.M.), and Division of Pediatric Cardiology, Department of Pediatric and Adolescent Medicine (S.J.A.), Mayo Clinic Medical Scientist Training Program (C.L.), Mayo Clinic, Rochester, MN; and Leviev Heart Center, Sheba Medical Center, Sackler School of Medicine, Tel Aviv University, Tel Aviv, Israel (E.M.).

*Mr Livia and Dr Sugrue are co-first authors.

Correspondence to: Christopher J. McLeod, MBChB, PhD, Heart Rhythm Services, Cardiovascular Department, Mayo Clinic, Rochester, MN 55902. E-mail: mcLeod.christopher@mayo.edu

Received March 5, 2018; accepted June 21, 2018.

© 2018 The Authors. Published on behalf of the American Heart Association, Inc., by Wiley. This is an open access article under the terms of the Creative Commons Attribution-NonCommercial-NoDerivs License, which permits use and distribution in any medium, provided the original work is properly cited, the use is non-commercial and no modifications or adaptations are made.

Clinical Perspective

What Is New?

- This study investigated the potential role of irreversible electroporation (IRE) to target the Purkinje fibers, which are thought to play an important role in the triggering and maintenance of ventricular fibrillation.
- In 8 acute canine experiments, IRE could ablate the Purkinje fiber signals in a dose-dependent and relatively safe manner.
- Abolishing Purkinje signals with IRE was associated with a decreased window of vulnerability toward ventricular fibrillation induction.

What Are the Clinical Implications?

- IRE potentially represents a novel safe method to ablate Purkinje fibers without significant damage to underlying myocardium.
- IRE of Purkinje fibers is a promising approach and requires further study for the treatment of ventricular fibrillation.

electroporation (IRE) is applied. IRE is attractive because it does not rely on thermal energy for tissue ablation and has been effective in multiple different models experimentally and clinically to destroy noncardiac tissue.^{12–15} More recently, proof-of-concept models have demonstrated successful electrical isolation of the pulmonary veins in large animal experiments with tissue IRE.^{16–18}

We aimed to, therefore, demonstrate Purkinje/fascicular fiber elimination via a nonthermal IRE approach. We hypothesized that the subendocardial Purkinje fibers could be destroyed with relative sparing of the myocardial contractile cells on the basis of electroporation parameters. Also, we assessed whether the functional elimination of the left ventricular Purkinje fibers affected the threshold/vulnerability for VF.

Methods

Data can be made available to other researchers by request to the corresponding author.

Animal and Heart Preparation

The Mayo Clinic Animal Care and Use Committee approved this study. A total of 8 mongrel dogs (weight, 25–40 kg) underwent cardiectomy under deep sedation with general anesthesia. In brief, after anesthesia, a left lateral thoracotomy allowed for visualization of the heart and great vessels. After full heparinization, the aorta was ligated and cannulated, with subsequent cardioplegia administration. Once asystole

was achieved, the heart was immediately cooled to 4°C. The heart was then explanted and placed on a Langendorff perfusion rig.¹⁹ The ex vivo functioning of the hearts was maintained using a large animal Langendorff apparatus (Radnoti, Monrovia, CA). The hearts were perfused using a modified Krebs-Henseleit solution oxygenated and buffered with 95% O₂ and 5% CO₂.²⁰ The perfusate solution consisted of the following: NaCl (118 mmol/L), D-glucose (11 mmol/L), KH₂PO₄ (1.18 mmol/L), KCl (4.7 mmol/L), MgSO₄ (1.17 mmol/L), CaCl₂ (2.0 mmol/L), NaHCO₃ (25 mmol/L), mannitol (16 mmol/L), sodium pyruvate (2.3 mmol/L), and human insulin (Novolin; Novo Nordisk, Plainsboro, NJ) (10 U/L of solution). The temperature of the perfusate was maintained at 37°C±1°C.

Electrophysiological Mapping

Detailed 3-dimensional electroanatomical mapping of the left ventricle via direct insertion of catheters through the left atrium and mitral valve was performed using the CARTO Mapping System (Biosense Webster, Inc, Diamond Bar, CA). Intracardiac mapping was performed using a Navistar ablation catheter with a 3.5-mm tip and electrode spacing of 2–5–2 mm (Biosense Webster). Three-dimensional electroanatomical maps were created, and mapping was performed in the ventricle, in addition to annotation of the His bundle, as well as fascicular and Purkinje signals. Fascicular potentials were labeled if a high-frequency electrogram occurred before the ventricular electrogram but with a short isoelectric period intervening. Purkinje potentials were derived from the noninsulated portion of the conduction system, which were recognized by no isoelectric period between the high-frequency Purkinje potential and the ventricular electrogram. The left bundle was assumed to be a direct extension of the His potential, without any atrial electrogram visible on the proximal pair of electrodes.

Determination of Window of Vulnerability

A shock on T-wave approach was used to determine the vulnerability of each heart to VF. A standard endocardial implantable cardioverter defibrillator lead (Medtronic, Minneapolis, MN) with a dual-coil defibrillator (Medtronic) was screwed into the right ventricular apex, as per standard convention in the human, and the superior vena cava coil was draped around the lateral wall of the left ventricle. Biphasic shocks were delivered between the 2 coils, and the implantable cardioverter defibrillator generator was excluded from the shocking vector. The window of vulnerability was assessed by initially defining the lower limit and subsequently the upper limit of VF inducibility via a shock on T-wave method.^{11,21,22} A 1-J shock stimulus (S2) was delivered at 260 ms after a drive train of 8 ventricular paced stimuli. If VF

could not be induced, the T wave was then scanned in 10-ms decrements/increments until the vulnerable S2 timing was identified. After identification of the ideal S2 interval that reliably induced VF (3 consecutive inductions), the intensity of the shock was adjusted lower in 0.2-J decrements until VF was no longer inducible. The lowest shock intensity able to reliably induce VF was then defined as the lower limit of vulnerability. The upper limit of vulnerability was then defined using the same drive train and S2 interval after the drive train, and stepping down from 35 J in 5-J (to 25 J) and then in 1-J decrements until VF could again be reliably induced with a shock delivered on the T wave. These same parameters were then used after electroporation to identify whether ablation had altered this measure. If VF could not be induced, then the lower limit of vulnerability was redefined by increasing the shock intensity in 0.2-J increments, and the upper limit of vulnerability was defined by reducing the shock intensity in 1-J decrements until VF was again induced. The S2 interval remained constant after initial definition.

Direct Current IRE

Irreversible electroporation was synchronized with the QRS and delivered using the NanoKnife system (AngioDynamics, Queensbury, NY). Using a modified 8-mm radiofrequency ablation catheter, 10 pulses at escalating voltages were delivered to the beating ex vivo heart at a frequency of 1 Hz; the pulse duration was kept constant at 90 μ s. The energy was delivered in a unipolar manner to a grounding pad that was submerged in the Langendorff bath, and adjacent to the left ventricular epicardial surface (at an approximate distance of <3 cm from the delivery catheter). The site of delivery was deliberately chosen to be nearby and not in contact with the Purkinje potentials mapped using the electroanatomical mapping catheter. The electroporation catheter was consistently kept between 10 and 25 mm from the mapping catheter and the target Purkinje/fascicle tissue. The mapping catheter was not moved away from the Purkinje tissue during electroporation (Figure 1).

Catheter Visualization

In the absence of fluoroscopy, catheter position was followed in real time and distances between mapping and ablation catheters were confirmed using direct visualization. This was possible in the context of the transparent Krebs-Henseleit solution using a 4.1-mm laryngovideoscope (ENDO-EYE Flexible Intubation; Olympus, Center Valley, PA) (Figure 1).

Statistical Analysis

Statistical analyses were performed using JMP, version 10 (SAS Institute, Cary, NC). Continuous variables are expressed

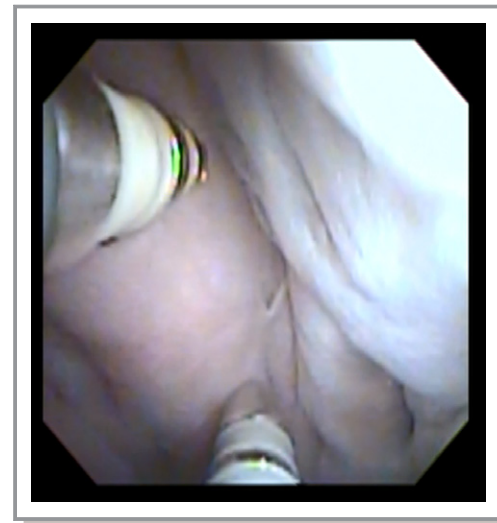


Figure 1. Endoscopic view of the left ventricular endocardium, demonstrating both the mapping catheter and ablation catheter separated by at least 10 to 25 mm.

as mean \pm SEM. Paired Student *t* test was used to compare both the differences in myocardial amplitude and VF window of vulnerability before and after delivery of ablation. A 2-tailed $P<0.05$ was considered significant.

Results

Effect of DC IRE on Purkinje and Fascicular Potentials

Electroporation energy was delivered to tissue at 750, 1000, 1500, 2000, or 2500 V (with a minimal electric field strength of 250, 333, 500, 666, and 833 V/cm, respectively), in a train of 10 pulses at 1 Hz, with each pulse having a duration of 90 μ s. The presence of the Purkinje potential was recorded using the mapping catheter before and after delivery of DC energy. Across all voltages used, the Purkinje potential was eradicated (Table 1, Figure 2). At the lowest energy deliveries of 750 and 1000 V (\approx 250–333 V/cm), the Purkinje potential was initially abolished but was noted to recur at the 5-minute time point (Table 1). The left bundle potential could not be abolished until a second delivery at 2000 V (\approx 666 V/cm) was reached. The His bundle could not be ablated at any energy delivery up to and including 2500 V (\approx 833 V/cm). In 4 hearts, at 2500 V, we noted complete but transient heart block with a ventricular escape rhythm. Conduction resumed within 3 to 8 minutes.

Effect of DC Electroporation on Left Ventricular Myocardial Tissue

Evaluation of the ventricular electrogram amplitude was performed immediately after ablation. Any immediate

Table 1. IRE Delivery Parameters and Presence of Purkinje Potentials

Animal No.	Voltage Delivered, V	Pulse Duration, μ s	Pulse No.	Pulse Frequency, Hz	Presence of Purkinje Potentials		Left Bundle Potential	His Potential
					1 Min	5 Min		
1	750	90	10	1	—	+	+	+
2	750	90	10	1	—	+	+	+
3	1000	90	10	1	—	+	+	+
4	1000	90	10	1	—	+	+	+
5	1500	90	10	1	—	—	+	+
6	2000	90	10	1	—	—	+	+
7	2000	90	10	1	—	—	—	+
8	2500	90	10	1	—	—	—	+

+ Indicates present; —, absent; IRE, irreversible electroporation.

deleterious effect on myocardial conduction properties adjacent to the Purkinje/fascicle tissue was noted and recorded (Table 2). The mean ventricular electrogram signal amplitude was 3.8 ± 1.8 mV before ablation and 3.2 ± 1.8 mV at 1 minute after electroporation ablation. The mean difference was a reduction in amplitude of -0.6 ± 2.3 mV ($P=0.03$).

VF Vulnerability

As reflected in Table 3 and Figure 3, at baseline, the initial lower limit of vulnerability to VF was 1.8 ± 0.4 J, and the upper limit of vulnerability was 19.5 ± 3.0 J, with a window of vulnerability of 17.8 ± 2.9 J. Delivery of electroporation energy to the Purkinje fibers resulted in the inability to induce VF in 4 animals. There was a significant reduction observed in the window of vulnerability (5.7 ± 2.9 J, $P=0.0003$), with a postablation lower limit of vulnerability= 7.3 ± 2.63 J, and the upper limit of vulnerability= 18.8 ± 5.2 J.

Discussion

This study identifies a novel approach for the ablation of fascicular and Purkinje fibers in an ex vivo beating heart model and highlights many novel observations. First, IRE can successfully eradicate Purkinje tissue both reversibly and irreversibly, in what appears to be a dose-dependent manner. Second, as evidenced by the maintenance of the integrity and amplitude of the ventricular signal, the IRE field can be manipulated to minimize ventricular myocardial damage. Third, the short-term eradication of Purkinje potentials within the left ventricular endocardial surface was also associated with a reduction in the window of vulnerability toward VF induction. Last, IRE does not appear to be contact dependent compared with current thermal-based energy sources.

Purkinje and Fascicular Ablation

The widespread nature of the short-term electroporative/ablative effect of IRE portends to provide a significant advancement over current catheter-based myocardial ablation techniques, particularly radiofrequency and cryoablation. Contemporary modalities are typically composed of point-by-point radiofrequency or cryotherapy ablation for ventricular arrhythmia ablation. Given the incredible redundancy and arborizing nature of Purkinje fibers,²³ coupled with the trabeculated nature of the left ventricle, an approach using electroporation may be a promising alternative. Consistent with other noncardiac electroporation patterns of injury, the extent of injury found was not solely reliant on contact and confined to the tissue adjacent to the catheter tip, but a result of the electric field (V/cm) created.^{24–27} The ablation electrode was deliberately kept at least 10 mm (and up to 25 mm) away from the Purkinje that was being actively recorded. DC was then pulsed between the catheter tip and the grounding pad adjacent to the left ventricular epicardial surface (at a maximal distance of 3 cm). Mechanisms behind this observed noncontact effect are not entirely clear, but we hypothesize that the ionic nature of the Krebs-Henseleit solution likely acted as a conductor of DC in this model, facilitating a virtual electrode footprint of injury. It is unclear whether blood will do the same, given the particulate and cellular components. If this is further proved, it highlights a truly invaluable aspect of IRE. Similarly, mapping of Purkinje-related arrhythmias is also notoriously difficult,²⁸ in lieu of the complex anatomical features, and this method of ablation may also remove the need for detailed mapping. Thereby, the case length and complexity are decreased, and safety is potentially increased, with a potential for improved efficacy.

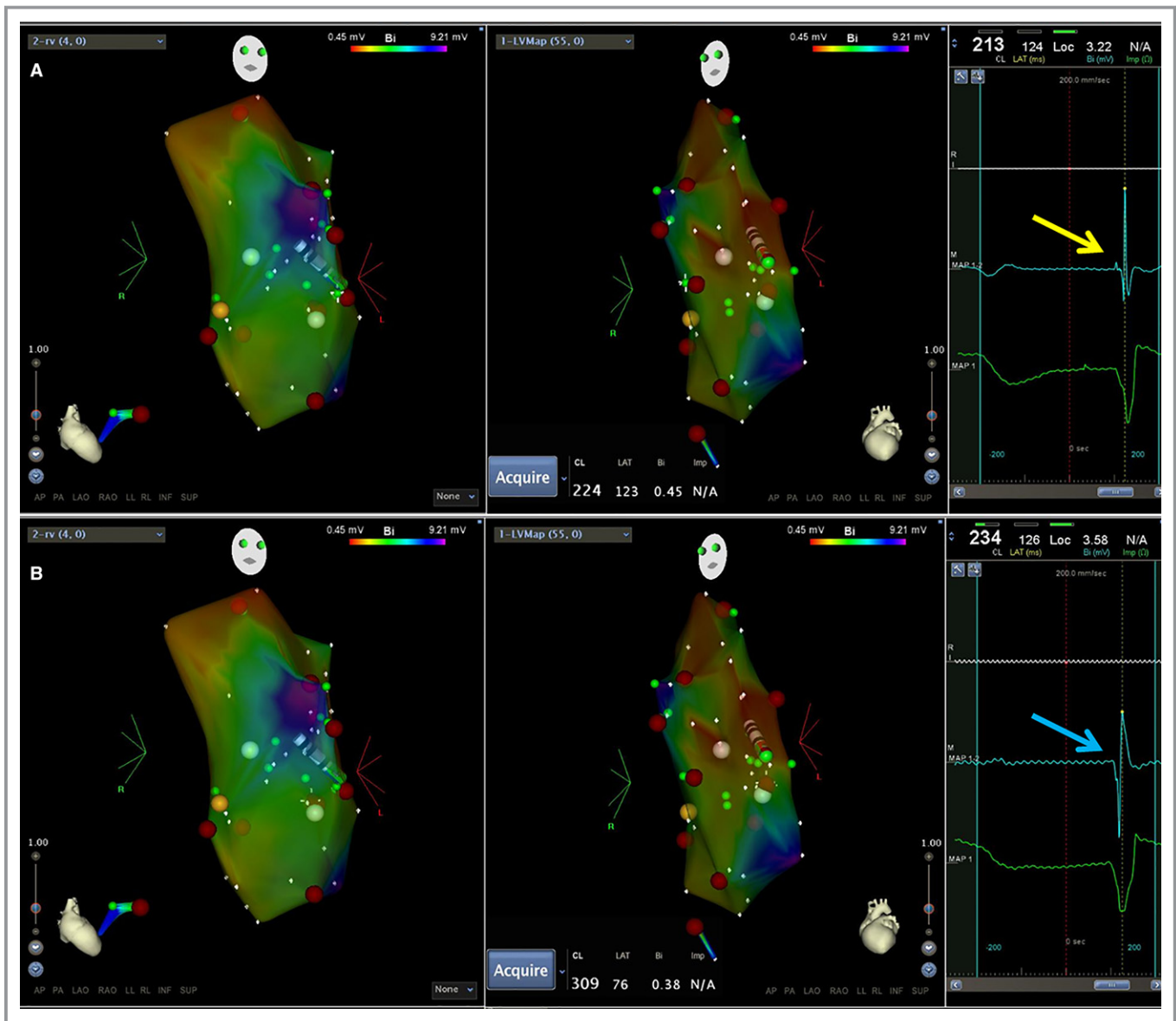


Figure 2. Representative electroanatomical map before (A) and after (B) electroporation. The fascicular/Purkinje signal is well seen before direct current delivery of 1000 V and electroporation (yellow arrow). The electroanatomical map showed that the mapping catheter has not moved. Yet, the fascicular signal is no longer present (blue arrow). Furthermore, the electrogram amplitude is essentially unchanged.

Reversible Electroporation and IRE

Although reversible electroporation has many applications in the medical field, gene transfer,²⁹ and electrochemotherapy,^{30,31} it is IRE that garnishes much attention and interest and has been harnessed as a clinical tool in the management of noncardiac pathological conditions.^{13,32–35} The findings of this investigation recapitulate the ability of electroporation to produce both reversible and irreversible effects on tissue. It has been well described that the electric field (V/cm) can be manipulated to exert different effects on tissue. Electrical pulses may vary in their shape, voltage, duration, and polarity. Voltage, duration of the pulse, and the distance between the delivery probes (ie, electric field strength) are the most

influential parameters in electroporation. This is shown in our work: as we increased the electric field strength (ie, V/cm) delivered, we observed a greater electroporative effect. Varying these parameters gives the opportunity to target tissue selectively.^{36–39} In our case, with some manipulation of the electric field (namely, the voltage delivered), we did not observe any myocardial damage. Further evaluation of different electric field parameters will be important.

The nonthermal nature of this technique provides a significant safety advantage by reducing the risk of collateral damage, which commonly occurs during ablation, especially if being used in the heart, where selective injury can target the tissue of interest yet potentially avoid coronary arteries^{40,41} or

Table 2. Myocardial Amplitude Before and After Delivery of IRE

Animal No.	Average Myocardial Amplitude, mV		
	Before Delivery	1-Min After Delivery	Difference
1	3.1±2.4	1.6±1.0	-1.5±1.9
2	8.4±4.1	6.8±4.2	-1.6±3.8
3	2.9±0.7	2.8±1.8	-0.1±1.9
4	2.7±1.8	2.0±1.5	-0.7±0.3
5	3.2±2.5	3.0±3.2	-0.1±1.8
6	2.9±2.4	2.0±1.5	-0.6±0.3
7	3.1±1.1	2.6±1.0	-0.5±1.1
8	4.7±1.7	4.9±4.5	0.3±4.2
Mean±SEM	3.8±1.8	3.2±1.8	-0.6±2.3*

Data are given as mean±SEM. IRE indicates irreversible electroporation.
**P* = 0.03.

extracardiac structures.^{38,42,43} Furthermore, stroke risk may also putatively be reduced because of the lack of coagulum formation, with electroporation compared with the heating that occurs with radiofrequency. In addition, our group has shown that DC fields applied during radiofrequency energy delivery can prevent the formation of coagulum on the catheter tip.⁴⁴

Efficiency could also be significantly enhanced given that electroporation can be performed in seconds to minutes (compared with several hours with radiofrequency ablation). This concept is especially important in scenarios where large surfaces of the ventricle need to be treated to eliminate Purkinje fibers, and a prolonged ablation is a higher risk procedure for the sicker patient.

To date, successful applications of IRE to cardiac tissue, in addition to the pulmonary veins, includes the coronary vessels,^{40,41} phrenic nerve,⁴² and ganglia.⁴⁵ Apart from the novel application of IRE to Purkinje fibers, our study does

support the work of others in that DC can be delivered to the beating heart. Delivery of energy during the vulnerable electrical period during cardiac repolarization can trigger VF. However, delivery of energy in this investigation was gated to the QRS, and VF was not induced by ablation.⁴⁶

Reducing the Window of Vulnerability Toward VF Induction

The role of the Purkinje system in the initiation and maintenance of VF is well established.⁴⁷⁻⁴⁹ In animal models targeting the Purkinje system, there has been a consistent demonstration of improved resilience toward VF^{11,50} and polymorphic ventricular arrhythmias.⁵¹ On the basis of this reasoning, a window of vulnerability to VF was assessed via a shock-on-T-wave phenomenon. The findings suggest a higher threshold toward VF induction, yet it is difficult to know whether this surrogate is a clinically meaningful result. VF could not be induced by ventricular extrastimulation protocols in this series of experiments, using single double and triple extrastimuli at 2 different drive trains (down to 160 ms), yet high-frequency bursting was not assessed. An ideal surrogate for VF susceptibility has not been agreed on. Different electrical stimulation techniques and methods have been proposed and tested, such as a restitution protocol,⁵² single-pulse stimulation,⁵³⁻⁵⁷ and 60-Hz alternating current stimulation.^{55,56,58,59}

Limitations

Although we have shown a short-term effect of IRE on the Purkinje fibers, subsequent study in a survived animal must be performed to determine whether an enduring effect is seen and to demonstrate clinical efficacy. Electroporation is field strength dependent, relying on both the voltage delivered and

Table 3. Window of Vulnerability Before and After IRE Delivery

Animal No.	Before Ablation			After Ablation		
	Lower VF Vulnerability	Upper VF Vulnerability	VF Window	Lower VF Vulnerability	Upper VF Vulnerability	VF Window
1	0.6	15	14.4	0*
2	0.6	20	19.4	0*
3	1	8	7	3	8	5
4	3	25	22	5	12	7
5	1	15	14	0*
6	3	13	10	0*
7	3	25	22	15	25	10
8	2	35	33	6	30	24
Mean±SEM	1.8±0.4	19.5±3.0	17.7±2.9	7.3±2.7	18.5±5.2	5.75±2.9

IRE indicates irreversible electroporation; VF, ventricular fibrillation.
*VF not inducible.

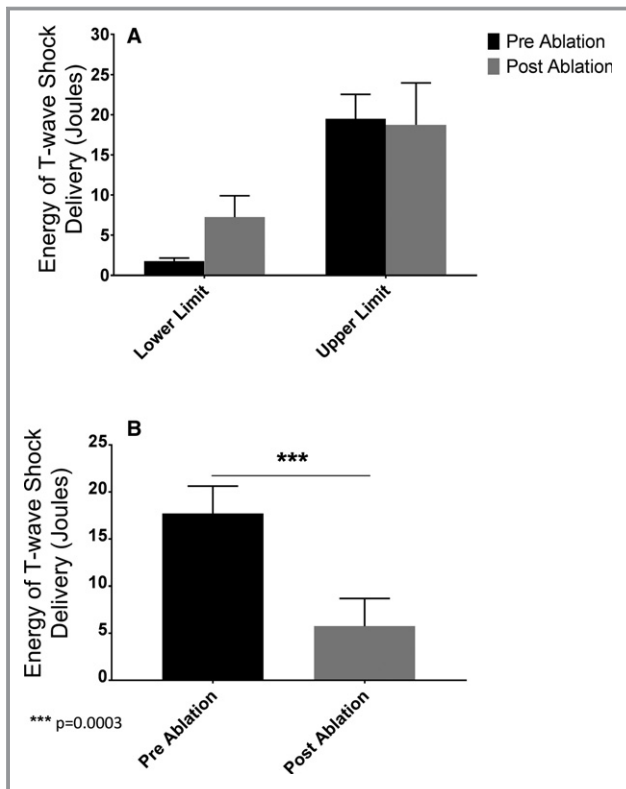


Figure 3. Vulnerability to ventricular fibrillation. A, Limits of vulnerability showing both the upper and lower limits. B, Window of vulnerability.

the distance this voltage is applied over. In our study, this distance was always <3 cm; however, the nature of the Langendorff setup and Krebs bath means that there will be some variability between catheter and grounding pad and, therefore, it is difficult to be exact in this measurement. Consequently, we have provided in this article the minimum predicted electric field strength that we delivered. We did not formally evaluate ventricular function with echocardiography or strain imaging or perform pathological analysis to assess the impact of IRE. In addition, although IRE is considered nonthermal^{60–62} at higher voltages (specifically, 2500 V), we cannot rule out the possibility of a local increase in temperature. Another major limitation also relates to the different conduction properties between the Krebs buffer as opposed to blood, and whether this can be extrapolated to the human is unclear and merits further study. Last, whether delivering a shock on a T wave is a true measure of VF tolerance and intolerance remains controversial,^{63–66} and although unlikely, the implantable cardioverter defibrillator shocks themselves could have been a confounder.

Conclusion

In a large-animal ex vivo beating heart model, our findings suggest that IRE can ablate the Purkinje signals in a dose-

dependent and relatively safe manner. The underlying cardiac muscle does not fibrillate if gated appropriately to the QRS, and the left ventricular myocardium does not appear substantially injured. Furthermore, abolishing Purkinje signals in the heart seems to be associated with an improved resistance toward VF induction. These findings hold major promise for this approach in ablating Purkinje-related arrhythmias, such as VF.

Disclosures

None.

References

- de Luna AB, Coumel P, Leclercq JF. Ambulatory sudden cardiac death: mechanisms of production of fatal arrhythmia on the basis of data from 157 cases. *Am Heart J*. 1989;117:151–159.
- Wood MA, Stambler BS, Damiano RJ, Greenway P, Ellenbogen KA. Lessons learned from data logging in a multicenter clinical trial using a late-generation implantable cardioverter-defibrillator. *J Am Coll Cardiol*. 1994;24:1692–1699.
- Hayashi M, Shimizu W, Albert CM. The spectrum of epidemiology underlying sudden cardiac death. *Circ Res*. 2015;116:1887–1906.
- Wellens HJ, Schwartz PJ, Lindemans FW, Buxton AE, Goldberger JJ, Hohnloser SH, Huikuri HV, Kääh S, La Rovere MT, Malik M. Risk stratification for sudden cardiac death: current status and challenges for the future. *Eur Heart J*. 2014;35:1642–1651.
- Haissaguerre M, Shah DC, Jais P, Shoda M, Kautzner J, Arentz T, Kalushe D, Kadish A, Griffith M, Gaita F, Yamane T, Garrigue S, Hocini M, Clementy J. Role of Purkinje conducting system in triggering of idiopathic ventricular fibrillation. *Lancet*. 2002;359:677–678.
- Nogami A, Sugiyasu A, Kubota S, Kato K. Mapping and ablation of idiopathic ventricular fibrillation from the Purkinje system. *Heart Rhythm*. 2005;2:646–649.
- Haissaguerre M, Shoda M, Jais P, Nogami A, Shah DC, Kautzner J, Arentz T, Kalushe D, Lamaison D, Griffith M, Cruz F, de Paola A, Gaita F, Hocini M, Garrigue S, Macle L, Weerasooriya R, Clementy J. Mapping and ablation of idiopathic ventricular fibrillation. *Circulation*. 2002;106:962–967.
- Lopera G, Stevenson WG, Soejima K, Maisel WH, Koplan B, Sapp JL, Satti SD, Epstein LM. Identification and ablation of three types of ventricular tachycardia involving the His-Purkinje system in patients with heart disease. *J Cardiovasc Electrophysiol*. 2004;15:52–58.
- Santoro F, Di Biase L, Hranitzky P, Sanchez JE, Santangeli P, Perini AP, Burkhardt JD, Natale A. Ventricular fibrillation triggered by PVCs from papillary muscles: clinical features and ablation. *J Cardiovasc Electrophysiol*. 2014;25:1158–1164.
- Knecht S, Sacher F, Wright M, Hocini M, Nogami A, Arentz T, Petit B, Franck R, De Chillou C, Lamaison D, Farre J, Lavergne T, Verbeet T, Nault I, Matsuo S, Leroux L, Weerasooriya R, Cauchemez B, Lellouche N, Derval N, Narayan SM, Jais P, Clementy J, Haissaguerre M. Long-term follow-up of idiopathic ventricular fibrillation ablation: a multicenter study. *J Am Coll Cardiol*. 2009;54:522–528.
- Damiano RJ Jr, Smith PK, Tripp HF Jr, Asano T, Small KW, Lowe JE, Ideker RE, Cox JL. The effect of chemical ablation of the endocardium on ventricular fibrillation threshold. *Circulation*. 1986;74:645–652.
- Sutter O, Calvo J, N'Kontchou G, Nault JC, Ourabia R, Nahon P, Ganne-Carrie N, Bourcier V, Zentar N, Bouhafs F, Sellier N, Diallo A, Seror O. Safety and efficacy of irreversible electroporation for the treatment of hepatocellular carcinoma not amenable to thermal ablation techniques: a retrospective single-center case series. *Radiology*. 2017;284:877–886.
- Fruhling P, Nilsson A, Duraj F, Haglund U, Noren A. Single-center nonrandomized clinical trial to assess the safety and efficacy of irreversible electroporation (IRE) ablation of liver tumors in humans: short to mid-term results. *Eur J Surg Oncol*. 2017;43:751–757.
- Valerio M, Dickinson L, Ali A, Ramachandran N, Donaldson I, McCartan N, Freeman A, Ahmed HU, Emberton M. Nanoknife electroporation ablation trial: a prospective development study investigating focal irreversible electroporation for localized prostate cancer. *J Urol*. 2017;197:647–654.

15. Vogel JA, Rombouts SJ, de Rooij T, van Delden OM, Dijkgraaf MG, van Gulik TM, van Hooft JE, van Laarhoven HW, Martin RC, Schoorlemmer A, Wilmsink JW, van Lienden KP, Busch OR, Besselink MG. Induction chemotherapy followed by resection or irreversible electroporation in locally advanced pancreatic cancer (IMPALA): a prospective cohort study. *Ann Surg Oncol*. 2017;24:2734–2743.
16. Neven K, van Driel V, van Wessel H, van Es R, Doevendans PA, Wittkamp F. Epicardial linear electroporation ablation and lesion size. *Heart Rhythm*. 2014;11:1465–1470.
17. Wittkamp FH, van Driel VJ, van Wessel H, Neven KG, Grundeman PF, Vink A, Loh P, Doevendans PA. Myocardial lesion depth with circular electroporation ablation. *Circ Arrhythm Electrophysiol*. 2012;5:581–586.
18. van Driel VJ, Neven KG, van Wessel H, du Pre BC, Vink A, Doevendans PA, Wittkamp FH. Pulmonary vein stenosis after catheter ablation: electroporation versus radiofrequency. *Circ Arrhythm Electrophysiol*. 2014;7:734–738.
19. McLeod CJ, Jeyabalan AP, Minners JO, Clevenger R, Hoyt RF, Sack MN. Delayed ischemic preconditioning activates nuclear-encoded electron-transfer-chain gene expression in parallel with enhanced postanoxic mitochondrial respiratory recovery. *Circulation*. 2004;110:534–539.
20. Krebs HA, Henseleit K. Untersuchungen über die Harnstoffbildung im Tierkörper. *Hoppe-Seyler's Zeitschrift für physiologische Chemie*. 1932;210:33–66.
21. Horowitz LN, Spear JF, Moore EN. Relation of the endocardial and epicardial ventricular fibrillation thresholds of the right and left ventricles. *Am J Cardiol*. 1981;48:698–701.
22. Fisher J, Sonnenblick EH, Kirk ES. Increased ventricular fibrillation threshold with severe myocardial ischemia. *Am Heart J*. 1982;103:966–972.
23. Boyden PA, Dun W, Robinson RB. Cardiac Purkinje fibers and arrhythmias: the GK Moe Award Lecture 2015. *Heart Rhythm*. 2016;13:1172–1181.
24. Miklavčić D, Beravs K, Šemrov D, Cemažar M, Demšar F, Serša G. The importance of electric field distribution for effective in vivo electroporation of tissues. *Biophys J*. 1998;74:2152–2158.
25. Garcia PA, Davalos RV, Miklavčić D. A numerical investigation of the electric and thermal cell kill distributions in electroporation-based therapies in tissue. *PLoS One*. 2014;9:e103083.
26. Lee YJ, Lu DS, Osuagwu F, Lassman C. Irreversible electroporation in porcine liver: acute computed tomography appearance of ablation zone with histopathologic correlation. *J Comput Assist Tomogr*. 2013;37:154–158.
27. Neal RE, Millar JL, Kavnoudias H, Royce P, Rosenfeldt F, Pham A, Smith R, Davalos RV, Thomson KR. In vivo characterization and numerical simulation of prostate properties for non-thermal irreversible electroporation ablation. *Prostate*. 2014;74:458–468.
28. Asirvatham SJ. The challenges of trigger ablation for ventricular fibrillation. *J Cardiovasc Electrophysiol*. 2015;26:116–117.
29. Neumann E. Membrane electroporation and direct gene transfer. *Bioelectrochem Bioenerg*. 1992;28:247–267.
30. Silve A, Mir LM. Cell Electroporation and Cellular Uptake of Small Molecules: The Electrochemotherapy Concept. In: Kee S, Gehl J, Lee E. (eds) *Clinical Aspects of Electroporation*. New York, NY: Springer; 2011.
31. Mali B, Jarm T, Snoj M, Sersa G, Miklavčić D. Antitumor effectiveness of electrochemotherapy: a systematic review and meta-analysis. *Eur J Surg Oncol*. 2013;39:4–16.
32. Diehl SJ, Rathmann N, Kostrzewa M, Ritter M, Smakic A, Schoenberg SO, Kriegmair MC. Irreversible electroporation for surgical renal masses in solitary kidneys: short-term interventional and functional outcome. *J Vasc Interv Radiol*. 2016;27:1407–1413.
33. Van den Bos W, de Bruin DM, Muller B, Varkarakis I, Karagiannis A, Zondervan P, Pes ML, Veelo D, Heijink CS, Engelbrecht M. The safety and efficacy of irreversible electroporation for the ablation of prostate cancer: a multicentre prospective human in vivo pilot study protocol. *BMJ Open*. 2014;4:e006382.
34. Ting F, Tran M, Böhm M, Siriwardana A, Van Leeuwen P, Haynes A, Delprado W, Shnier R, Stricker P. Focal irreversible electroporation for prostate cancer: functional outcomes and short-term oncological control. *Prostate Cancer Prostatic Dis*. 2016;19:46–52.
35. Vroomen LG, Scheffer HJ, Melenhorst MC, de Jong MC, van den Bergh JE, van Kuijk C, van Delft F, Kazemier G, Meijerink MR. MR and CT imaging characteristics and ablation zone volumetry of locally advanced pancreatic cancer treated with irreversible electroporation. *Eur Radiol*. 2017;27:2521–2531.
36. Davalos RV, Mir L, Rubinsky B. Tissue ablation with irreversible electroporation. *Ann Biomed Eng*. 2005;33:223–231.
37. Rubinsky J, Onik G, Mikus P, Rubinsky B. Optimal parameters for the destruction of prostate cancer using irreversible electroporation. *J Urol*. 2008;180:2668–2674.
38. Maor E, Ivorra A, Leor J, Rubinsky B. The effect of irreversible electroporation on blood vessels. *Technol Cancer Res Treat*. 2007;6:307–312.
39. Li W, Fan Q, Ji Z, Qiu X, Li Z. The effects of irreversible electroporation (IRE) on nerves. *PLoS One*. 2011;6:e18831.
40. du Pré BC, van Driel VJ, van Wessel H, Loh P, Doevendans PA, Goldschmeding R, Wittkamp FH, Vink A. Minimal coronary artery damage by myocardial electroporation ablation. *Europace*. 2012;15:144–149.
41. Neven K, van Driel V, van Wessel H, van Es R, du Pré B, Doevendans PA, Wittkamp F. Safety and feasibility of closed chest epicardial catheter ablation using electroporation. *Circ Arrhythm Electrophysiol*. 2014;7:913–919.
42. van Driel VJ, Neven K, van Wessel H, Vink A, Doevendans PA, Wittkamp FH. Low vulnerability of the right phrenic nerve to electroporation ablation. *Heart Rhythm*. 2015;12:1838–1844.
43. Neven K, van Es R, van Driel V, van Wessel H, Fidler H, Vink A, Doevendans P, Wittkamp F. Acute and long-term effects of full-power electroporation ablation directly on the porcine esophagus. *Circ Arrhythm Electrophysiol*. 2017;10:e004672.
44. Lim B, Venkatachalam K, Henz BD, Johnson SB, Jahangir A, Asirvatham SJ. Prevention of coagulum formation with simultaneous charge delivery in radiofrequency ablation: a canine model. *JACC Clin Electrophysiol*. 2016;2:233–241.
45. Madhavan M, Venkatachalam K, Swale MJ, Desimone CV, Gard JJ, Johnson SB, Suddendorf SH, Mikell SB, Ladewig DJ, Nosbush TG. Novel percutaneous epicardial autonomic modulation in the canine for atrial fibrillation: results of an efficacy and safety study. *Pacing Clin Electrophysiol*. 2016;39:407–417.
46. Deodhar A, Dickfeld T, Single GW, Hamilton WC Jr, Thornton RH, Sofocleous CT, Maybody M, Gonen M, Rubinsky B, Solomon SB. Irreversible electroporation near the heart: ventricular arrhythmias can be prevented with ECG synchronization. *AJR Am J Roentgenol*. 2011;196:W330–W335.
47. Nogami A. Mapping and ablating ventricular premature contractions that trigger ventricular fibrillation: trigger elimination and substrate modification. *J Cardiovasc Electrophysiol*. 2015;26:110–115.
48. Huang J, Dossdall DJ, Cheng K-A, Li L, Rogers JM, Ideker RE. The importance of Purkinje activation in long duration ventricular fibrillation. *J Am Heart Assoc*. 2014;3:e000495. DOI: 10.1161/JAHA.113.000495.
49. Haissaguerre M, Vigmond E, Stuyvers B, Hocini M, Bernus O. Ventricular arrhythmias and the His-Purkinje system. *Nat Rev Cardiol*. 2016;13:155–166.
50. Dossdall DJ, Tabereaux PB, Kim JJ, Walcott GP, Rogers JM, Killingsworth CR, Huang J, Robertson PG, Smith WM, Ideker RE. Chemical ablation of the Purkinje system causes early termination and activation rate slowing of long-duration ventricular fibrillation in dogs. *Am J Physiol*. 2008;295:H883–H889.
51. Caref EB, Boutjdir M, Himel HD, El-Sherif N. Role of subendocardial Purkinje network in triggering torsade de pointes arrhythmia in experimental long QT syndrome. *Europace*. 2008;10:1218–1223.
52. Luo Q, Jin Q, Zhang N, Huang S, Han Y, Lin C, Ling T, Chen K, Pan W, Wu L. Antifibrillatory effects of renal denervation on ventricular fibrillation in a canine model of pacing-induced heart failure. *Exp Physiol*. 2018;103:19–30.
53. Cha Y-M, Peters BB, Birgersdotter-Green U, Chen P-S. A reappraisal of ventricular fibrillation threshold testing. *Am J Physiol*. 1993;264:H1005–H1010.
54. Wiggers CJ, Wégria R. Ventricular fibrillation due to single, localized induction and condenser shocks applied during the vulnerable phase of ventricular systole. *Am J Physiol*. 1940;128:500–505.
55. Fabritz CL, Kirchhof PF, Behrens S, Zabel M, Franz MR. Myocardial vulnerability to T wave shocks: relation to shock strength, shock coupling interval, and dispersion of ventricular repolarization. *J Cardiovasc Electrophysiol*. 1996;7:231–242.
56. Bhandari AK, Isber N, Estioko M, Ziccardi T, Cannom DS, Park Y, Lerman RD, Prejean C, Sun G-W. Efficacy of low-energy T wave shocks for induction of ventricular fibrillation in patients with implantable cardioverter defibrillators. *J Electrocardiol*. 1998;31:31–37.
57. Swerdlow CD, Martin DJ, Kass RM, Davie S, Mandel WJ, Gang ES, Chen PS. The zone of vulnerability to T wave shocks in humans. *J Cardiovasc Electrophysiol*. 1997;8:145–154.
58. Voroshilovsky O, Qu Z, Lee M-H, Ohara T, Fishbein GA, Huang H-LA, Swerdlow CD, Lin S-F, Garfinkel A, Weiss JN. Mechanisms of ventricular fibrillation induction by 60-Hz alternating current in isolated swine right ventricle. *Circulation*. 2000;102:1569–1574.
59. Panitchob N, Li L, Huang J, Ranjan R, Ideker RE, Dossdall DJ. Endocardial activation drives activation patterns during long-duration ventricular fibrillation and defibrillation. *Circ Arrhythm Electrophysiol*. 2017;10:e005562.
60. Maor E, Ivorra A, Rubinsky B. Non thermal irreversible electroporation: novel technology for vascular smooth muscle cells ablation. *PLoS One*. 2009;4:e4757.

61. Golberg A, Yarmush ML. Nonthermal irreversible electroporation: fundamentals, applications, and challenges. *IEEE Trans Biomed Eng.* 2013;60:707–714.
62. Daniels C, Rubinsky B. Electrical field and temperature model of nonthermal irreversible electroporation in heterogeneous tissues. *J Biomech Eng.* 2009;131:071006.
63. Chen PS, Shibata N, Dixon EG, Martin RO, Ideker RE. Comparison of the defibrillation threshold and the upper limit of ventricular vulnerability. *Circulation.* 1986;73:1022–1028.
64. Hou CJ, Chang-Sing P, Flynn E, Martinez L, Peterson J, Ottoboni LK, Liem LB, Sung RJ. Determination of ventricular vulnerable period and ventricular fibrillation threshold by use of T-wave shocks in patients undergoing implantation of cardioverter/defibrillators. *Circulation.* 1995;92:2558–2564.
65. Swerdlow CD, Davie S, Ahern T, Chen PS. Comparative reproducibility of defibrillation threshold and upper limit of vulnerability. *Pacing Clin Electrophysiol.* 1996;19:2103–2111.
66. Hwang C, Swerdlow CD, Kass RM, Gang ES, Mandel WJ, Peter CT, Chen PS. Upper limit of vulnerability reliably predicts the defibrillation threshold in humans. *Circulation.* 1994;90:2308–2314.